Magnetospheric Multiscale Observation of Plasma Velocity-Space Cascade: Hermite Representation and Theory

S. Servidio, A. Chasapis, W. H. Matthaeus, D. Perrone, F. Valentini, T. N. Parashar, P. Veltri, D. Gershman, C. T. Russell, B. Giles, S. A. Fuselier, T. D. Phan, and J. Burch

Phys. Rev. Lett. **119**, 205101 — Published 16 November 2017

DOI: 10.1103/PhysRevLett.119.205101

Magnetospheric Multiscale (MMS) observation of plasma velocity-space cascade: Hermite representation and theory

S. Servidio[1], A. Chasapis[2], W. H. Matthaeus[2], D. Perrone[3], F. Valentini[1], T. N. Parashar[2], P. Veltri[1], D. Gershman[4], C. T. Russell[5], B. Giles[4], S. A. Fuselier[6], T. D. Phan[7], J. Burch[5]

[1]*Dipartimento di Fisica, Università della Calabria, I-87036 Cosenza, Italy*

[2]*Bartol Research Institute and Department of Physics and Astronomy, University of Delaware, Newark, DE 19716, USA*

[3]*European Space Agency, ESAC, Madrid, Spain*

[4]*NASA Goddard Space Flight Center, Greenbelt, MD, USA*

[5] *University if California at Los Angeles*

[6]*Southwest Research Institute, San Antonio, TX, USA*

[7]*University of California, Berkeley, CA, USA*

(Dated: October 9, 2017)

Plasma turbulence is investigated using unprecedented high-resolution ion velocity distribution measurements by the Magnetospheric Multiscale Mission (MMS) in the Earth's magnetosheath. This novel observation of a highly structured particle distribution suggests a cascade-like process in velocity space. Complex velocity space structure is investigated using a three-dimensional Hermite transform, revealing, for the first time in observational data, a power law distribution of moments. In analogy to hydrodynamics, a Kolmogorov approach leads directly to a range of predictions for this phase-space transport. The scaling theory is found to be in agreement with observations. The combined use of state-of-the-art MMS datasets, novel implementation of a Hermite transform method, and scaling theory of the velocity cascade, opens new pathways to understanding of plasma turbulence and the crucial velocity space features that lead to dissipation in plasmas.

Turbulence in fluids is characterized by nonlinear interactions that transfer energy from large to small scales, eventually producing heat. For a collisional medium, whether an ordinary gas or a plasma, turbulence leads to complex real space structure, but the velocity space, constrained by collisions, remains smooth and close to local thermodynamic equilibrium (as, e.g., in Chapman-Enskog theory [1].) However, in a weakly collisional plasma, spatial fluctuations are accompanied by fluctuations in velocity space, representing another essential facet of plasma dynamics. The characterization of the velocity space is challenging in computations and in experiments, although recent Vlasov simulation has revealed velocity space complexity, often found near real-space coherent structures [2–6]. Here we demonstrate an analysis of new, highly accurate spacecraft data in the terrestrial magnetosheath that quantifies the velocity cascade for the first time in a space plasma. This methodology fills an essential gap in our understanding of the final steps of plasma dynamics that lead to dissipation and heating.

The observations reported here are enabled by the Magnetospheric Multiscale Mission (MMS), launched in 2015 to explore magnetic reconnection. The MMS/FPI instrument measures ion and electron velocity distributions (VDFs) at high time cadence, and with high resolution in angle and energy. High resolution measurement and four-point observation is available for all instruments. MMS characterizes plasma turbulence with unprecedented resolution and accuracy, as the spacecraft orbit repeatedly crosses the Earth's magnetosheath (see e.g. Burch et al. [7]). Here we focus on one traversal of the magnetosheath, and specifically on a quantitative description of the ion velocity space cascade.

Magnetosheath data sample. The analysis below employs data from the period 2016-01-11, 00:57:04 to 2016-01-11, 01:00:33, about five hours after an outbound magnetosheath crossing, and four hours before the next inbound crossing. Apogee is $\approx$12 *Re* at 02:16:54. The spacecraft, separated by $\sim$ 40km ($\sim \frac{1}{2} - 1$ ion gyroradius) are downstream of the quasi-parallel bow shock, and the interplanetary magnetic field is nearly radial. In such conditions, fully developed upstream turbulence readily convects into the magnetosheath, The selected interval contains fine scale activity including sub-proton scale current sheets, as previously described by Chasapis et al. [10]. The magnetic field in this period is highly turbulent as shown in Figure 1-(a). **For more background, see the Supplemental Material [8].**

In this fairly typical compressive magnetosheath interval [9], large values of plasma beta $\beta \sim 7$ and the large ratio of rms fluctuations to mean field strength, $\delta b/B_0 \sim 1.5$, indicates near-isotropy of turbulence statistics. The magnetic field power spectrum **(see [8])** is consistent with Kolmogorov scaling in wavenumber $k \approx 2\pi f/V$ (bulk flow speed V), with a $k^{-5/3}$ slope at low frequency $f < 0.8$ Hz, and a steeper $k^{-8/3}$ spectrum at higher frequencies, similar to the solar wind case [11]. Coherent structures are present in the analyzed interval [3, 4, 10, 12, 13] and these are associated with enhanced nonMaxwellian kinetic activity.

Our analysis concentrates on the ion velocity distribution functions (VDFs) $f(\boldsymbol{v}, t)$, measured by identical FPI instruments on each MMS spacecraft MMS$_i$ ($i = 1, .., 4$).

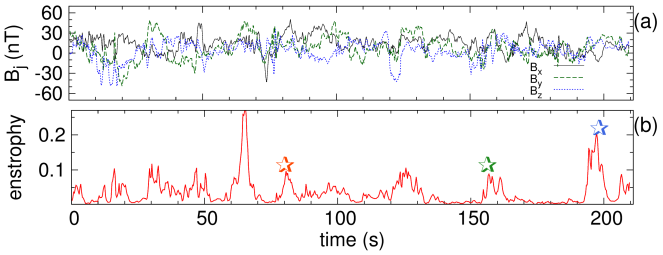

FIG. 1: Sample of MMS data, plotted vs. time (seconds), beginning at 2016-01-11, 00:57:04 in the magnetosheath. (a) Magnetic field components; (b) Enstrophy. Stars indicate selected times at which we show ion VDFs in Fig. 2. The analyses will refer to this time axis.

FPI time resolution for ion VDFs is $\Delta t = 150$ ms, for the entire burst interval duration of $\sim$ 210 seconds. **The VDFs are collected in the spacecraft frame in spherical geometry, $f(v, \phi, \theta, t)$. Here ϕ is the azimuthal angle ($0 < \phi < 2\pi$), θ the angle with the z (spin) axis ($0 < \theta < \pi$), and $40 < v < 2400$ km/s. At its highest time resolution, FPI samples 32 energy channels, and an interleaved set of 32 energy channels at the following time. Merging consecutive data samples allows construction of a VDF with effectively double the energy resolution, 64 energy channels, but with reduction of the time cadence by half, to 300 ms. We use the merged, higher energy-resolution data in the analysis below, with N =64 log-spaced energy channels, $N_\phi = 32$ and $N_\theta = 16$ equally sampled angular channels. Using this increased energy resolution data also reduces velocity space data gaps.**

Hermite analysis method. We employ a 3D Hermite transform representation of $f(\boldsymbol{v}, t)$, a method well-suited for analytical and numerical study of plasmas [14–17]. The "physicists" Hermite polynomials are defined as $H_m(v) = (-1)^m e^{v^2} \frac{d^m}{dv^m} e^{-v^2}$, orthogonal in a Hilbert space where the metric is defined by the Maxwellian weight function e^{-v^2}. The one-dimensional basis functions are

$$\psi_m(v) = \frac{H_m\left(\frac{v-u}{v_{th}}\right)}{\sqrt{2^m m! \sqrt{\pi} v_{th}}} e^{-\frac{(v-u)^2}{2v_{th}^2}}, \qquad (1)$$

where u and v_{th} are the bulk velocity and the thermal speed, respectively, and $m \geq 0$ is an integer.

The eigenfunctions in Eq. (1) obey the orthogonality condition $\int_{-\infty}^{\infty} \psi_m(v)\psi_l(v)dv = \delta_{ml}$. Using this basis, one can obtain a 3D decomposition of the distribution function

$$f(\boldsymbol{v}) = \sum_{\boldsymbol{m}} f_{\boldsymbol{m}} \psi_{\boldsymbol{m}}(\boldsymbol{v}), \qquad (2)$$

where the 3D eigenfunctions are $\psi_{\boldsymbol{m}}(\boldsymbol{v}) = \psi(m_x, v_x)\psi(m_y, v_y)\psi(m_z, v_z)$, and the Hermite coefficients are

$$f_{\boldsymbol{m}} = \int_{-\infty}^{\infty} f(\boldsymbol{v})\psi_{\boldsymbol{m}}(\boldsymbol{v})d^3v. \qquad (3)$$

Note that, in the case of a Maxwellian, $f(v) = M(v) = e^{-v^2/2}$ and the first coefficient $f_{\boldsymbol{0}} = \frac{n}{\left[2v_{th}\sqrt{\pi}\right]^{3/2}}$. This simple case gives a deep meaning to the Hermite projection in plasmas, namely that each Hermite index m roughly corresponds to an order of the plasma moments: the $m = 1$ coefficient corresponds to bulk flow fluctuations; $m = 2$ corresponds to temperature deformations; $m = 3$ to heat flux perturbations, and so on. This suggests that highly deformed VDFs would produce a distribution of modes.

MMS analysis. We now perform a Hermite analysis of the MMS data. We adopt a 3D non-uniform grid in each direction based on the zeroes v_j of the Hermite polynomial of order $N_v + 1$, $[H_{N_v+1}(v_j) = 0; j = 0, N_v + 1]$. For these results, we choose $N_v \equiv N_{v_x} = N_{v_y} = N_{v_z} = 100$. This spans a velocity space, centered at zero speed, defined by the $N_v + 1$ values of $v_j; j = 0, N_v$ [18]. The velocity is normalized in terms of the local thermal velocity $v_{th}(t)$, the density is normalized such that $n(t) = 1$, and the local fluid velocity $\boldsymbol{u}(t) = 0$ is built into the representation (velocity is measured relative to the bulk fluid frame). This normalization is performed at each (300ms cadence) time snapshot of the ion VDF, for each spacecraft MMS_i. Values of $f(\boldsymbol{v})$ are transformed from the native (MMS) spherical representation to the non-uniform (Cartesian) grid, using a 2^{nd} order interpolation method, weighting with volumes $V = \int_{v_1}^{v_2} \int_{\theta_1}^{\theta_2} \int_{\phi_1}^{\phi_2} v^2 sin\theta \; dvd\theta d\phi$ within each angular sector of the MMS data grid. We tested the accuracy of the interpolation technique by comparing the case with 64 energy channels and 32 energy channels; these differ by negligible amounts for $m < 20$. This procedure produces a normalized VDF on a new "Hermite grid", $f(v_x, v_y, v_z)$, where velocities are in units of local thermal speed, with $\boldsymbol{u} = 0$, and unit density. The occurrence of missing data points is reduced by averaging $f(\boldsymbol{v})$ over the separate measurements on the four MMS satellites. The effect of this averaging is discussed below and in [8].

Following this procedure results in a three dimensional rendering of the interpolated VDF at a single time ($t \sim 80$ s in Fig. 1), illustrated in Fig. 2. The distribution is highly non-Maxwellian, the pictorial representation already suggesting a broad spectrum of moments. The same figure shows 2D cuts of the interpolated VDF, at several different times: at $t = 80$ [same as panel (a); at $t = 156$; and at $t = 198$ s. Fig. 1 provides the context. It is evident that there are strong time-dependent non-Maxwellian deviations. Due to the high speed flow in the magnetosheath, one infers that such deformations are likely initiated by various local processes [4, 19].

In order to quantify deviations from fluids, we compute the mean square departure from Maxwellianity, equivalent to the second Casimir invariant of the VDF,

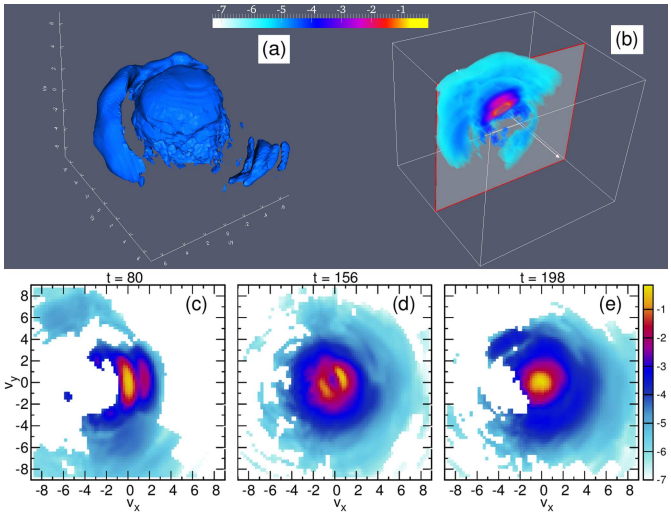

FIG. 2: (a) Ion velocity distribution function, obtained from the MMS mission interpolating the function over a Hermite grid (data from $t = 80$ s in Fig.1) and averaging over the 4 satellites. (b) 2D cut in the v_x, v_y plane, with 3D shaded contours. Panels (c), (d) and (e) represents slices of the VDF at different times, highlighted with stars in Fig. 1-(c).

which has been to called the enstrophy in analogy to the mean square vorticity in hydrodynamics [20]. We define the local deviation from the associated Maxwellian $\delta f = f(v) - M(v)$, a procedure equivalent to subtracting f_0 from the Hermite series. Note that $M(v)$ is the Maxwellian at each time t, and that δf is therefore the deviation from local equilibrium. Using this projection, the Parseval theorem gives the enstrophy

$$\Omega(t) \equiv \int_{-\infty}^{\infty} \delta f^2(\boldsymbol{v}, t) d^3v = \sum_{\boldsymbol{m}>0} \left[f_{\boldsymbol{m}}(t)\right]^2 . \qquad (4)$$

This quantity is zero for a pure Maxwellian, and may be compared with other measures of non-Maxwellianity in plasma turbulence studies [4]. It is also related to what is designated the "'free energy" in certain reduced perturbative treatments of kinetic plasma (e.g., [21]). The plasma enstrophy as a function of time is reported in Fig. 1-(b). Its behavior is quite bursty, and is qualitatively connected to spatial intermittency in the system [4–6]. The distributions shown above in Fig. 2 correspond to the times of local peaks of $\Omega(t)$ seen in Fig. 1-(b).

Following Eq. 3, and using the above normalization and averaging procedures for the VDF data, we compute the modal 3D Hermite spectrum $f^2_{\boldsymbol{m}}(t)$. **We emphasize that this spectrum is not explicitly influenced by variations in local bulk flow, temperature or density.** For an ensemble average description of the entire sample, our method averages the multidimensional Hermite spectra of the shifted distributions over time, indicating this as $E(m_x, m_y, m_z) = \langle f^2_{\boldsymbol{m}}(t)\rangle_T$. The 3D modal spectrum (as in Fourier analysis) permits examination of the full 3D structure of the spectral distribution. Given the great volume of data, it may be reduced or sampled to attain more compact representations. To this end, we compute the reduced 2D spectra as $E(m_x, m_y) = \sum_{m_z} E(m_x, m_y, m_z)$, and analogously $E(m_x, m_z)$ and $E(m_y, m_z)$. Figure 3 shows two of these reduced spectra. Within their respective planes, these spectra are quite isotropic, indicating the lack of preferred direction in the ensemble when referred to the spacecraft frame. **This leaves open the question as to whether there are local preferred directions associated with quantities such as magnetic field or shear within this stream. This will be examined at a later time, but we do not anticipate a strong magnetic field influence, given the large values of $\delta b/B_0$ and β.**

Based on the 2D spectra, a reasonable way to characterize the velocity space fluctuations for this dataset is the isotropic velocity space spectrum. The isotropic (omni-directional) Hermite spectrum, in analogy to the classical spectral density in hydrodynamic turbulence, is computed by summing $E(m_x, m_y, m_z)$ over concentric shells of thickness δ (here, unity) in the Hermite index space. That is, $P(m) = \sum_{m-\frac{1}{2}<|\mathbf{m}'|\leq m+\frac{1}{2}} E(\mathbf{m}')$.

The isotropic Hermite spectrum of magnetosheath turbulence is reported in Fig. 3-(c). The velocity space distribution follows a power law behavior through at least the first ten moments, indicating the possibility of a phase-space turbulent cascade, as suggested in the literature [17, 21–27]. In particular, an important work by Schekochihin *et al.* presents a set of expectations for this velocity-space cascade, in the context of drift-wave turbulence. **Various tests have been performed to examine the robustness of the analysis presented here. The adopted normalizations avoid unwanted interference by routine fluid-like variations of the zeroth, first and second moments. We found that the apparent spectral break for $m > 12$, is not influenced by the noise level, the interpolation technique, and the statistical uncertainty due to lack of data. Fluctuations in the first few moments are a familiar feature in spectral analysis, and is fractionally greater in the noise data. The spectrum in Fig. 3-(c) has also been computed from single MMS spacecraft data, obtaining the same results for $m < 12$; for further discussion. See Supplemental Material [8] for additional discussion of these issues. Additional technical analyses will also be presented elsewhere.**

The model. To develop an inertial range model of the observed spectrum $P(m) \sim m^{-\alpha}$, seen in Figure 3-(c) at $m < 15$, we develop a cascade theory based on qualitative arguments, in style similar to the Kolmogorov phenomenology [28]. The Boltzmann kinetic equation for weakly-collisional plasma,

$$\frac{\partial f}{\partial t} + \boldsymbol{\nabla}\cdot(\boldsymbol{v}f) + \frac{e}{M_p}\left(\boldsymbol{E} + \frac{\boldsymbol{v}}{c}\times\boldsymbol{B}\right)\cdot\boldsymbol{\nabla}_v f = C_\nu, \qquad (5)$$

couples to the Maxwell equations for the electric $\boldsymbol{E}$ and magnetic $\boldsymbol{B}$ field. M_p indicates the mass and e the charge

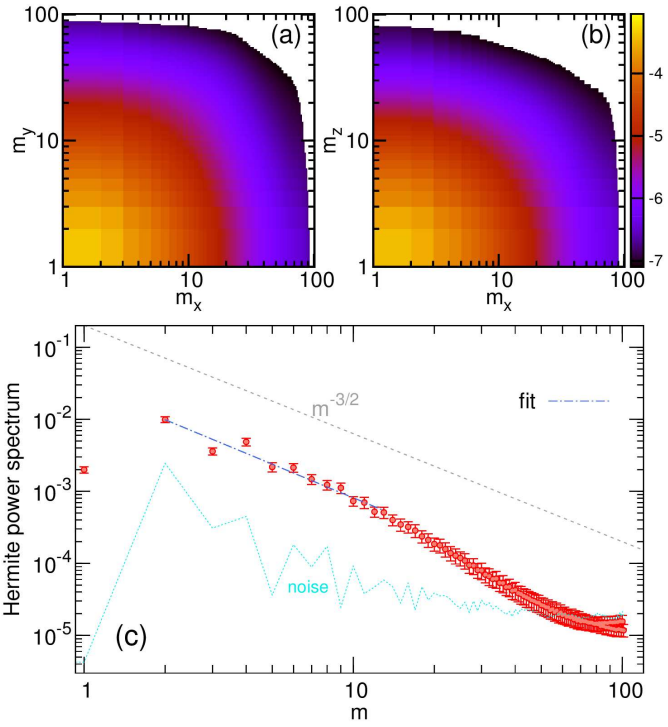

FIG. 3: (a) and (b): 2D reduced Hermite spectra, indicating near-isotropy in these two velocity space planes. (c) Ensemble (time-) averaged spectrum of the Hermite modes for the MMS dataset. The best fit to a power law (dash-dot line) $m^{-\alpha}$ gives $\alpha \sim 1.5$, with an error of $\sim 7\%$. Line with -3/2 slope (dashed) shown for reference. Error bars on data points are standard error of the mean. Noise floor (lower dotted line) is estimated using Hermite transform of randomized signal in velocity.

of ions. Eq. (5) includes a collision operator C_ν, which may have a complex form.

Upon computing the Hermite transform $[...]_m$ of Eq.(5), one arrives at a **fully equivalent** evolution equation for the coefficients $\frac{\partial f_{\boldsymbol{m}}(\boldsymbol{x},t)}{\partial t}$. Our approach is based on familiar assumptions employed in Navier-Stokes turbulence theory. We neglect collisions which are assumed to be confined to very high m Hermite modes. The crux of the procedure rests on estimating the timescales associated with the terms on the left hand side of Eq.(5). That is, we estimate three times scales $\tau_v(m)$, $\tau_E(m)$ and $\tau_B(m)$, such that $[\boldsymbol{\nabla}\cdot(\boldsymbol{v}f)]_m \sim f_m/\tau_v(m)$, $[\frac{e}{M_p}\boldsymbol{E}\cdot\boldsymbol{\nabla}_v f]_m \sim f_m/\tau_E(m)$ and $[\frac{e}{M_p}(\frac{\boldsymbol{v}}{c}\times\boldsymbol{B})\cdot\boldsymbol{\nabla}_v f]_m \sim f_m/\tau_B(m)$. An assumption of locality of scale in Hermite space is justified by recalling the Hermite recursion relations,

$$v\ \psi_m(v) = \sqrt{\frac{m}{2}}\psi_{m-1}(v) + \sqrt{\frac{m+1}{2}}\psi_{m+1}(v), \qquad (6)$$

$$\frac{\partial\psi_m(v)}{\partial v} = \sqrt{\frac{m}{2}}\psi_{m-1}(v) - \sqrt{\frac{m+1}{2}}\psi_{m+1}(v). \qquad (7)$$

From these we see that the couplings between Hermite modes in Eq.5 involve only local, nearest neighbors in m [26]. Both differentiation and multiplication by v introduce factors involving $\sqrt{m}$.

Proceeding, we envision three (asymptotic) regimes,

$$\frac{\partial f_m(t)}{\partial t} \sim \begin{cases} \frac{v_{th}}{d_i}\sqrt{m}\ f_m(t) & (a), \\ \frac{eE}{M_p v_{th}}\sqrt{m}\ f_m(t) & (b), \\ \frac{eB}{M_p c} m\ f_m(t) & (c), \end{cases} \qquad (8)$$

associated respectively with the dominance of each of the relevant terms in the Boltzmann equation. **In [case (a)] the dominant term is due to phase mixing and the spatial structure is assumed to have a characteristic scale $\sim d_i$; in [case (b)] the velocity space distortions are due to the electric field; in [case (c)] the dynamics is governed by the magnetic field.** Here E and B represent estimates of the r.m.s electric and magnetic field strengths. At larger scales $> d_i$, the ion inertial scale, one may approximate $E \sim \frac{\delta u}{c}B$. Other terms in the generalized Ohm's law may become dominant at scales $< d_i$, but we may assume for simplicity that the total electric field remains approximately continuous, so this simple estimate is retained. We recall that $d_i = V_A/\omega_{ci}$, V_A the Alfvén speed and $\omega_{ci} = eB/M_p c$ the ion cyclotron frequency.

Following some simple rearrangements, introducing the turbulent Mach number $M_t = \delta u/v_{th}$ and the plasma beta $\beta = v_{th}^2/V_A^2$, we extract from Eq. 8 three characteristic timescales:

$$\tau_v(m) = \frac{1}{\sqrt{\beta}\sqrt{m}}\ \omega_{ci}^{-1}, \qquad (9)$$

$$\tau_E(m) = \frac{1}{M_t\sqrt{m}}\ \omega_{ci}^{-1}, \qquad (10)$$

$$\tau_B(m) = \frac{1}{m}\ \omega_{ci}^{-1}. \qquad (11)$$

In all three regimes we expect redistribution of fluctuations in m-space, through a cascade/diffusion-like process. In the above we suppress the vector index $\mathbf{m}$, anticipating an isotropic theory for flux across shells in $|\mathbf{m}|$ as in a Kolmogorov approach.

At this stage, we adopt the hypothesis of an enstrophy cascade in the velocity space, based on the idea that velocity space transfer conserves the quadratic "rugged" invariant Ω, defined in Eq.(4). Thus, the first hypothesis is that of a net constant enstrophy flux in the m-space, namely

$$\epsilon = \frac{f_m^2}{\tau_m} = const, \qquad (12)$$

where τ_m is the spectral transfer time for the enstrophy. The second hypothesis concerns choice of the characteristic time of this cascade, the simplest options being to chose among (9)-(11). Finally, from simple dimensional

arguments,

$$\Omega = \langle \int \delta f^2 d^3v \rangle_x = \sum_{m>0} f_m^2 = \int P(m) dm, \\ \rightarrow P(m) \sim f_m^2 m^{-1}, \quad (13)$$

where we defined $\langle ... \rangle_x$ as the physical space volume average. Using Eq.s (12), (13) and a characteristic time, either (9) or (10), one finds

$$P(m) \sim m^{-3/2}. \quad (14)$$

Analogously, using Eq.s (12) and (13), coupled with the timescale in Eq. (11), one obtains

$$P(m) \sim m^{-2}. \quad (15)$$

The $-3/2$ powerlaw in Eq. (14) should be valid in a phase mixing or electric-field dominated regime, while the prediction of -2 in Eq. (15) is suitable for a highly magnetized plasma.

For the present observation, we fit an inertial range powerlaw to the velocity-space cascade, as shown in Figure 3-(c), obtaining $P(m) \sim m^{-\alpha}$, with $\alpha = 1.5 \pm 0.1$, in agreement with Eq. (14). This result is consistent with the characterization of this magnetosheath interval, which is relatively high beta (~ 7) and compressive [$M_t = O(1)$].

To conclude, we have carried out an analysis of MMS ion VDF data to visualize and describe the ion distribution function in this low-collisionality space plasma with unprecedented temporal and velocity-scale resolution. We observe here in spacecraft data the same kind of fine scale velocity structure reported frequently in Vlasov simulations [13, 19]. This motivates a further analysis of the velocity space structure in terms of a Hermite spectral analysis, which has the physically interesting interpretation as a moment hierarchy. The power law that emerges in moments (Hermite indices) suggests a velocity space cascade. We pursue this in a very preliminary way, in analogy to classical hydrodynamics cascade. One first identifies a conserved flux across scale – here the velocity space enstrophy (or, free energy) – and the associated dynamical time scales. From this emerges the possibility of spectral slopes between -2 and -3/2. Other possibilities may exist for other physical regimes in which different time scales become available. For the MMS magnetosheath interval analyzed here, the -3/2 slope seems to be clearly favored, suggesting that the velocity space cascade for this interval is governed by velocity advection (phase mixing) and/or electric effects [29]. In future works we will expand the current analysis to include additional datasets with varying plasma conditions, and Vlasov simulations, while also examining the influence of the local magnetic field and strong gradients.

This observation and analysis is preliminary, being based on a novel set of high resolution observations, and so we must eschew any assignment of universality. However, enabled by significant advances in diagnostics such as those offered by MMS, this approach to understanding velocity space structure may prove to be fruitful for further studies in turbulent plasmas, in varying conditions.

Acknowledgments

This research was partially supported by AGS-1460130 (SHINE), NASA grants NNX14AI63G (Heliophysics Grand Challenge Theory), the Solar Probe Plus science team (ISOIS/SWRI subcontract No. D99031L), and by the MMS Theory and Modeling team, NNX14AC39G. F. V. is supported by Agenzia Spaziale Italiana under contract ASI-INAF 2015-039-R.O. DP and SS acknowledge support from the Faculty of the European Space Astronomy Centre (ESAC). Computational support provided by the Newton cluster at UNICAL. **We are grateful to the MMS instrument teams, especially SDC, FPI, and FIELDS, for cooperation and collaboration in preparing the data. The data used in this analysis are Level 2 FIELDS and FPI data products, in cooperation with the instrument teams and in accordance their guidelines. All MMS data are available at https://lasp.colorado.edu/mms/sdc/.**

[1] K. Huang, *Statistical Mechanics* (1963).
[2] A. Greco, W. H. Matthaeus, S. Servidio, P. Chuychai, and P. Dmitruk, The Astrophys. J. Lett. **691**, L111 (2009).
[3] S. Servidio, F. Valentini, F. Califano, and P. Veltri, Physical Review Letters **108**, 045001 (2012).
[4] A. Greco, F. Valentini, S. Servidio, and W. Matthaeus, Physical Review E **86**, 066405 (2012).
[5] J. M. TenBarge and G. G. Howes, The Astrophys. J. Lett. **771**, L27 (2013).
[6] T. N. Parashar and W. H. Matthaeus, Astrophys. J. **832**, 57 (2016).
[7] J. L. Burch, T. E. Moore, R. B. Torbert, and B. L. Giles, Space Sci. Rev. **199**, 5 (2016).
[8] See Supplemental Material at http://link.aps.org/ for additional information on the fields of the dataset, the power spectrum of turbulence and the averaging procedure of the Hermite spectrum.
[9] D. Sundkvist, A. Retinó, A. Vaivads and S. D. Bale, Phys. Rev. Lett., **99**, 025004 (2007)
[10] A. Chasapis, W. H. Matthaeus, T. N. Parashar, O. LeContel, A. Retinò, H. Breuillard, Y. Khotyaintsev, A. Vaivads, B. Lavraud, E. Eriksson, et al., Astrophys. J. **836**, 247 (2017).
[11] F. Sahraoui, M. L. Goldstein, P. Robert, and Y. V. Khotyaintsev, Phys. Rev. Lett. **102** (2009).
[12] S. Servidio, K. T. Osman, F. Valentini, D. Perrone, F. Califano, S. Chapman, W. H. Matthaeus, and P. Veltri, The Astrophys. J. Lett. **781**, L27 (2014).
[13] S. Servidio, F. Valentini, D. Perrone, A. Greco, F. Cali-

fano, W. H. Matthaeus, and P. Veltri, Journal of Plasma Physics **81**, 325810107 (2015).
[14] H. Grad, Commun. Pure Appl. Math. **2**, 331 (1949).
[15] T. Armstrong and D. Montgomery, Journal of Plasma Physics **1**, 425 (1967).
[16] J. W. Schumer and J. P. Holloway, Journal of Computational Physics **144**, 626 (1998).
[17] J. T. Parker and P. J. Dellar, Journal of Plasma Physics **81**, 305810203 (2015).
[18] Y. Zhaohua, J. Comput. Phys. **258**, 371 (2014).
[19] G. G. Howes, K. G. Klein, and T. C. Li, Journal of Plasma Physics **83**, 705830102 (2017).
[20] G. Knorr, Plasma Physics **19**, 529 (1977).
[21] A. A. Schekochihin, S. C. Cowley, W. Dorland, G. W. Hammett, G. G. Howes, G. G. Plunk, E. Quataert, and T. Tatsuno, Plasma Physics and Controlled Fusion **50**, 124024 (2008).
[22] D. R. Hatch, F. Jenko, V. Bratanov, and A. Banon Navarro, J. Plasma Phys. **80**, 531 (2014).
[23] J. T. Parker, E. G. Highcock, A. A. Schekochihin, and P. J. Dellar, Physics of Plasmas **23**, 070703 (2016).
[24] N. J. Sircombe, T. D. Arber, and R. O. Dendy, Journal de Physique IV **133**, 277 (2006).
[25] T. Tatsuno, W. Dorland, A. A. Schekochihin, G. G. Plunk, M. Barnes, S. C. Cowley, and G. G. Howes, Physical Review Letters **103**, 015003 (2009).
[26] A. A. Schekochihin, J. T. Parker, E. G. Highcock, P. J. Dellar, W. Dorland, and G. W. Hammett, Journal of Plasma Physics **82**, 905820212 (2016).
[27] A. Kanekar, A. A. Schekochihin, W. Dorland, and N. F. Loureiro, Journal of Plasma Physics **81**, 305810104 (2015).
[28] A. Kolmogorov, Akademiia Nauk SSSR Doklady **30**, 301 (1941).
[29] F. Valentini and P. Veltri, Physical Review Letters **102**, 225001 (2009).